A Heuristic Algorithm for the Analysis of Fast Field Cycling (FFC) NMR Dispersion Curves

Journal:	*Analytical Chemistry*
Manuscript ID	Draft
Manuscript Type:	Letter
Date Submitted by the Author:	n/a
Complete List of Authors:	Lo Meo, Paolo; Universita degli Studi di Palermo, STEBICEF Terranova, Samuele; Universita degli Studi di Palermo, STEBICEF Di Vincenzo, Antonella; Università degli Studi di Palermo Dipartimento di Scienze e Tecnologie Biologiche Chimiche e Farmaceutiche Chillura Martino, Delia; Universita degli Studi di Palermo, STEBICEF Conte, Pellegrino; Universita degli Studi di Palermo, Dipartimento di Scienze Agrarie, Alimentari e Forestali

A Heuristic Algorithm for the Analysis of Fast Field Cycling (FFC) NMR Dispersion Curves.

Paolo Lo Meo,*[a] Samuele Terranova,[a] Antonella Di Vincenzo,[a] Delia Chillura Martino,[a] Pellegrino Conte.*[b]

[a]: Dipartimento di Scienze e Tecnologie Biologiche, Chimiche e Farmaceutiche (STEBICEF), University of Palermo; v.le delle Scienze pad. 17 – 90128 Palermo (Italy).

[b]: Dipartimento di Scienze Agrarie, alimentari e Forestali (SAAF), University of Palermo; v.le delle Scienze pad. 4 – 90128 Palermo (Italy).

ABSTRACT. Evaluation of NMRD curves obtained by the FFC-NMR relaxometric technique is a valuable tool for analyzing the microscopic dynamics of condensed matter systems. However, quantitative data analysis involves several conceptual and practical issues. Moving forward from previous literature approaches, we propose a new analysis method, relying on the elaboration of the inverse integral transform of the NMRD curve. Our approach results in a true heuristic method, able to unambiguously individuate the dynamic domains in the system, thereby avoiding the possible introduction of any element of discretion. Analysis of some datasets relevant to real samples, suggests the possibility that the results obtained with the heuristic method may be actually led back to some distinct physical/chemical features of the systems.

Fast-Field-Cycling (FFC) NMR relaxometry[1] is a powerful and versatile tool for investigating the molecular dynamics of condensed matter (either solid, amorphous or liquid, or even heterogeneous systems). This technique has found interesting applications in several fields, spanning from polymers and new materials, to soil and environmental science, as well as ionic liquids,[2] proteins,[3] dairy products,[4] and so on. However, a critical issue for its exploitation is the regression analysis of the NMRD dispersion curves, from which physically sensible information can be obtained.

The FFC technique evaluates how the longitudinal relaxation rate (R_1) or the relevant relaxation time ($T_1 = 1/R_1$) of a spinning nucleus varies on changing the strength of an applied magnetic field. According to the general theory developed by Bloch et al. for homonuclear dipolar relaxation,[5] R_1 depends on the nuclear Larmor frequency by the relationship:

$$R_1 = (T_1)^{-1} = K[\boldsymbol{J}_1(\omega_L) + 4\boldsymbol{J}_2(2\omega_L)] \quad (1)$$

Here J_1 and J_2 are the spectral density functions that, through the spin Hamiltonians, can be led back to the autocorrelation function of the relaxing nucleus. Hence, Bloembergen, Purcell and Pound derived the well-known relationship[6] (the so-called "BPP" model given in equation 2) for the proton relaxation in a simple system undergoing a single dynamical process:

$$R_1 = (T_1)^{-1} = \frac{3}{10}\frac{\mu_0^2\gamma^4}{\hbar^2 r_{HH}^6}\left(\frac{\tau_c}{1+(\omega_L\tau_c)^2} + \frac{4\tau_c}{1+4(\omega_L\tau_c)^2}\right) = C^{HH}\left(\frac{\tau_c}{1+(\omega_L\tau_c)^2} + \frac{4\tau_c}{1+4(\omega_L\tau_c)^2}\right) \quad (2)$$

where r_{HH} is the internuclear distance and τ_c is the *correlation time*, i.e. the average time needed for a molecule to rotate one radian or to move for a distance as large as its radius of gyration. The regression analysis of the NMRD dispersion curve enables to find valuable information on the microscopic dynamics of the system. Noticeably, in the range of low magnetic fields exploited by FFC, relaxation becomes faster as molecular motion slows down.

Dealing with complex systems is more complicated. In principle, based on equation 1, one should derive the exact expression for R_1 from the relevant autocorrelation function. Attempts in this sense can be found in literature. For instance, Korb et al. have treated the relaxometric behavior of proteins by a power-type law, developed assuming that relaxation can be rationalized in terms of spin-phonon interactions in a system where protons "*form a spin communication network described by a fractal dimension*".[7] Furthermore, Anoardo applied an approach, previously proposed by Torrey for the translational diffusion, to describe the behavior of viscous oils.[5b] Similar treatments are highly descriptive, but have an applicability limited only to specific systems. In alternative, "*model-free*" analyses have become quite popular. The conceptual issues of this approach have been clearly

described in his seminal papers by Halle,[8] who proposed the well-known mathematical treatment of NMRD curves (equation 3) as a linear combination of Lorentzian terms, the number of which must be discretionally/empirically set, i.e.:

$$R_1 = \frac{1}{T_1} = \sum_i \frac{c_i \tau_i}{1 + (\omega\tau_i)^2} \quad (3)$$

Here c_i are empirical weight coefficients, from which an average correlation time $\langle\tau_c\rangle$ can be calculated as: $\langle\tau_c\rangle = (\Sigma_i c_i\tau_i)/(\Sigma_i c_i)$. More recently, Kruk et al. proposed a valuable model free method for the analysis of NMRD profiles of proteins,[3] based on the following expression:

$$R_1(\omega_L) = R_0 + R^{HH} + R^{NH} \quad (4)$$

where R_0 is an offset keeping into account very "fast" molecular motions (τ_c < 1 ns), R^{HH} describes proper ^{1}H-^{1}H relaxation as a sum of three BPP-like components, i.e.:

$$R^{HH} = \sum_{i=1}^{3}\left[C_i^{HH}\left(\frac{\tau_i}{1+(\omega\tau_i)^2} + \frac{4\tau_{ci}}{1+4(\omega\tau_i)^2}\right)\right] \quad (5)$$

Finally, R^{NH} describes the occurrence of the so-called "quadrupolar dips", i.e. the sudden enhancement of the relaxation rate due to the quadrupolar coupling with ^{14}N (if present):

$$R^{NH} = C^{NH}\left[\begin{array}{l}\left(\frac{1}{3} + sen^2\Theta cos^2\Phi\right)\left(\frac{\tau_Q}{1+(\omega-\omega_-)^2\tau_Q^2} + \frac{\tau_Q}{1+(\omega+\omega_-)^2\tau_Q^2}\right) + \\ \left(\frac{1}{3} + sen^2\Theta sen^2\Phi\right)\left(\frac{\tau_Q}{1+(\omega-\omega_+)^2\tau_Q^2} + \frac{\tau_Q}{1+(\omega+\omega_+)^2\tau_Q^2}\right) + \\ \left(\frac{1}{3} + cos^2\Theta\right)\left(\frac{\tau_Q}{1+(\omega-(\omega_+-\omega_-))^2\tau_Q^2} + \frac{\tau_Q}{1+(\omega+(\omega_+-\omega_-))^2\tau_Q^2}\right)\end{array}\right] \quad (6)$$

where τ_Q is the correlation time for the N-H quadrupolar interaction, ω_+ and ω_- are the relevant characteristic frequencies, Θ and Φ are two angles accounting for "*the orientation of the ^{1}H–^{14}N dipole–dipole axis with respect to the principal axis system of the electric field gradient at the position of ^{14}N*";[2a] finally, the coefficient C^{NH} can be led back to the gyromagnetic ratios and the average interaction distance of the nuclei through the expression:

$$C^{NH} = \frac{2}{3}\cdot\frac{\mu_0^2\gamma_N^2\gamma_H^2}{\hbar^2 r_{NH}^6} \quad (7)$$

We have been recently interested in the FFC characterization of porous systems and, in particular, of nanosponges (NSs).[9] These interesting organic materials are hyper-reticulated polymers or co-polymers obtained by joining supramolecular host units (usually cyclodextrins, but also calixarenes or pillararenes) with suitable linker units.[10] Because of their permeability to aqueous media, NSs can find applications as sorbents for both organic and inorganic pollutants, drug carrier systems and functional supports for nanosized catalysts. Surprisingly, for various reasons their porosimetric/textural parameters can be hardly determined by BET/BJH techniques.[9a, 11] Therefore, based on similar studies in soil science,[12] from the FFC data of water-saturated NSs we succeeded in defining a suitable *porosimetric connectivity index* (*PCI*),[9a] able to quantify the functional permeability of the materials to aqueous media. Our previous study dealt with cyclodextrin-based materials reticulated with bis-urethane linker moieties. Therefore, their NMRD curves appeared ideal candidates to be treated by means of Kruk's equation. However, various problems have been encountered in performing such a regression analysis. In fact, the number *i* of BPP components in the second term (R^{HH}) of equation (4) cannot be fixed a priori to three, as in the original Kruk's approach, but must be adapted empirically. This, again, introduces an undesirable degree of discretion in data processing. It is worth mentioning here that the choice of three terms is not analytically justified in the reference study.[3a] A further problem arises from the fact that relative errors on R_1 are roughly constant along the explored ω_L range, whereas absolute errors are not. This treacherously involves that data recorded at the lowest magnetic field values are statistically overweighed, thereby affecting the convergence and the overall reliability of the fitting procedure.

In order to overcome the conceptual issues arising from the discretion degree of the model-free approaches, we considered the possibility to set up a new model-free-based regression procedure relying on Kruk's method. We reasoned that a complex system might be viewed as a continuum of different dynamic domains liable to be described in terms of a BBP-like function, each having its own τ_c value. Hence, a normalized distribution function $f(\tau_c)$ could be defined, which describes the overall microscopic dynamics of the system, and thus the term R^{HH} present in equation (5) can be transformed into an integral form as:

$$R^{HH} = \int_0^\infty\left[C^{HH}\left(\frac{\tau_c}{1+(\omega\tau_c)^2} + \frac{4\tau_c}{1+4(\omega\tau_c)^2}\right)\right]f(\tau_c)d\tau_c \quad (8)$$

Noticeably, according to equation 2, the coefficient C^{HH} should depend on the average internuclear interaction distance r_{HH}, which cannot be granted to be the same for different possible dynamic domains. Thus, r_{HH} should be considered as a function of τ_c, as well, and equation 8 can be re-formulated as:

$$R^{HH} = \int_0^\infty\left[\left(\frac{\tau_c}{1+(\omega\tau_c)^2} + \frac{4\tau_c}{1+4(\omega\tau_c)^2}\right)\right]f^*(\tau_c)d\tau_c \quad (9)$$

with $f^*(\tau_c) = C^{HH}\cdot f(\tau_c)$. Having available the function $R(\omega_L)$ defined by the experimental dataset, the problem reduces to retrieve an inverse integral transform, with the BPP-like term functioning as the kernel. From a mathematical standpoint, this is considered an "*ill-posed problem*",[13] hard to solve analytically. We tried to smartly approach it by setting up a home-made numerical integration procedure (further details are provided in the Supporting Information). In other words, the function $f^*(\tau_c)$ can be numerically built, in such a way that each calculated R_1 value achieves the best fit to the relevant experimental value, according to the well assessed criterion of the square residuals sum minimization. In doing this, the entire procedure must keep into account the simultaneous optimization of the offset R_0 and the six parameters relevant to the quadrupolar dips term R^{NH} (if ^{14}N is present in the

sample, i.e. C^{NH}, τ_Q, ω_+, ω_-, Φ and Θ). Moreover, in order to fix the problem of the possible statistical data overweighing, we conveniently defined the variable $\lambda_c = Log_{10}(\tau_c)$, and the function: $I^*(\lambda_c) = [2.303 \cdot 10^{\lambda c} \cdot f^*(10^{\lambda c})]^{1/2}$, in such a way to further transform the integral expression 9 into:

$$R^{HH} = \int_{-\infty}^{\infty} \left(\frac{10^{\lambda_c}}{1 + (\omega \cdot 10^{\lambda_c})^2} + \frac{4 \cdot 10^{\lambda_c}}{1 + 4(\omega \cdot 10^{\lambda_c})^2} \right) [I^*(\lambda_c)]^2 d\lambda_c \quad (10)$$

This ensures that the f^* function assumes only positive values. The function $I^*(\lambda_c)$ is finally built via numerical integration, with the aid of the algorithms implemented into the MS Excel™ software package, by applying the square residuals minimization criterion to $Log_{10}(R(\omega_L))$, i.e. in order to minimize the SSQ^* value defined as:

$$SSQ^* = \sum_i [Log(R(\omega_i)_{experim.}) - Log(R(\omega_i)_{clcd.})]^2 \quad (11)$$

We tested this approach on some selected datasets acquired from literature. In particular, we analyzed data relevant to: *i*) anhydrous β-cyclodextrin;[9a] *ii*) a dry nanosponge prepared by reacting anhydrous β-cyclodextrin with four equivalents of hexamethylene-bis-isocyanate;[9h] *iii*) a sample of 24-months aged Parmigiano Reggiano cheese.[4] Moreover, for useful comparison, we also collected and analyzed a dataset relevant to a sample of water-saturated commercial cellulose (data are reported in the Supporting Information). Results are illustrated in Figures 1-4.

As a first observation, in all the cases examined the obtained $[I^*(\lambda_c)]^2$ distribution functions (and thus the corresponding $f^*(\tau_c)$ functions) did not result into broad continuous curves, as it could have been reasonably expected, but rather into a set of very narrow distributions, or even Kronecker's delta-like peaks. The latter finding is particularly meaningful, because it implies that the $R(\omega_L)$ function defined by each experimental dataset can be actually transformed into a τ_c values spectrum. Thus, the proposed analysis constitutes a true heuristic algorithm, able to identify the dynamic domains that characterize the relaxometric behavior of the samples, the relevant τ_c values of which can be immediately deduced. Hence, the contributions to the NMRD curves pertaining to each dynamic domain, identified by the relevant τ_c peak, can be easily calculated (as depicted in the lower sections of Figures 1-4).

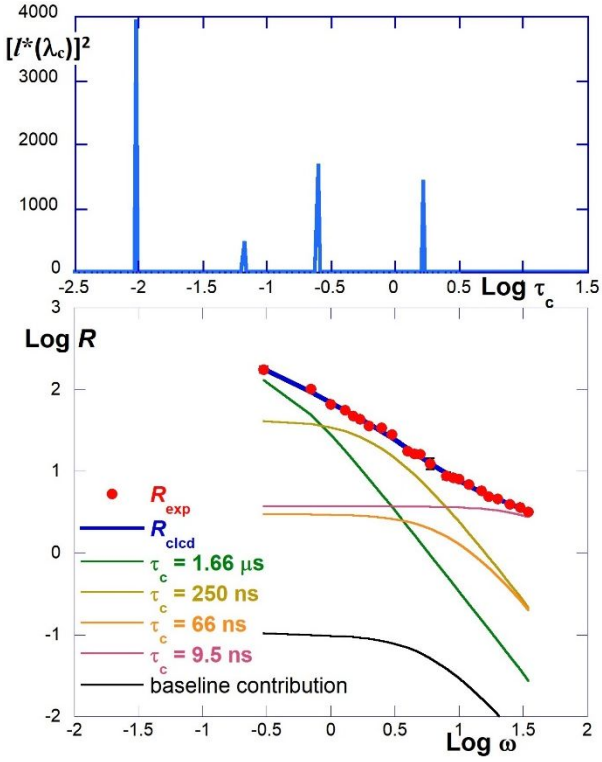

Figure 1. Spectrum of τ_c values (up) and NMRD curve (down) for the anhydrous β-cyclodextrin sample.

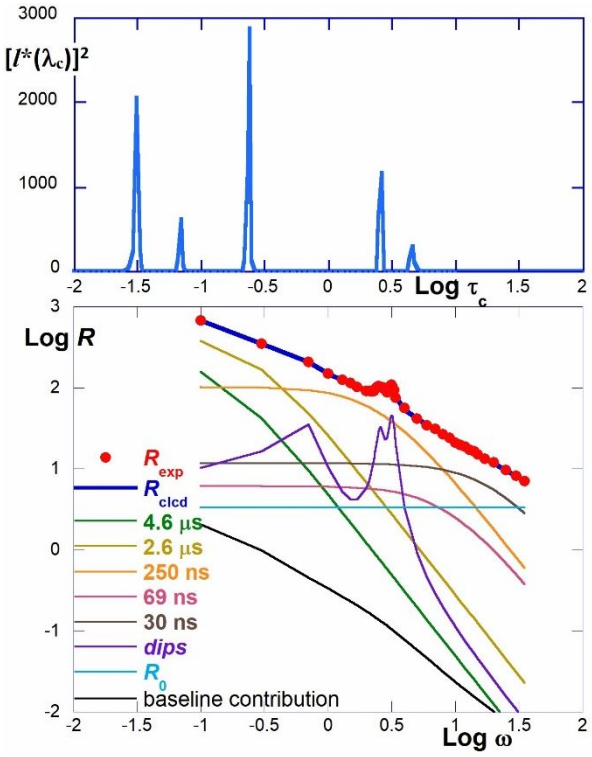

Figure 2. Spectrum of τ_c values (up) and NMRD curve (down) for the cyclodextrin-bis-urethane-based nanosponge sample.

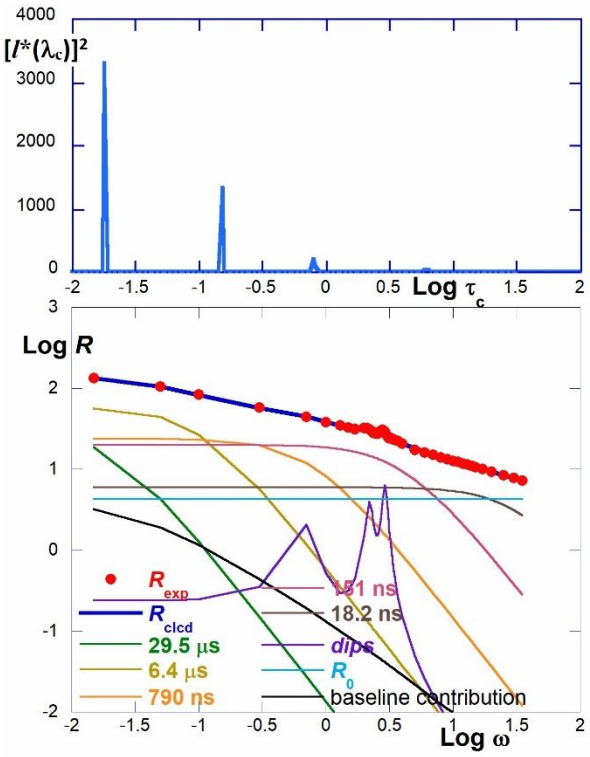

Figure 3. Spectrum of τ_c values (up) and NMRD curve (down) for the Parmigiano-Reggiano sample.

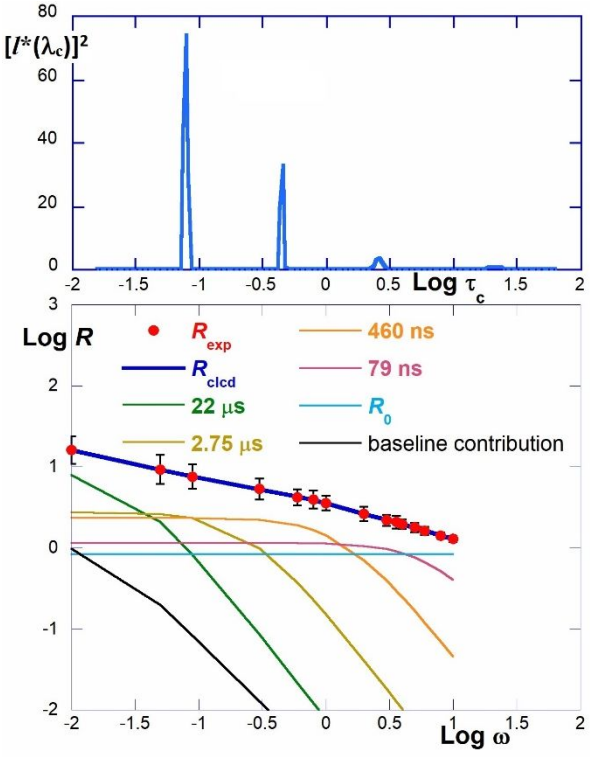

Figure 4. Spectrum of τ_c values (up) and NMRD curve (down) for the water saturated cellulose sample.

These considerations suggested the idea that the identified domains could be possibly related to distinct structural or physico-chemical features of the samples. However, before attempting such an analysis, some issues had to be addressed. In particular, we had to establish suitable criteria for estimating the indetermination on the τ_c values found (and the other regression parameters as well) and, in general, for assessing the reliability of the method, in order to identify possible artifacts. For this purposes, we exploited a Monte-Carlo approach[14] (see the Supporting Information for details) based on the generation of suitable virtual datasets, which were subjected to the same heuristic procedure described hereinabove. As a result, peak clusters were generated for each sample. These clusters, in turn, enable to unambiguously individuate as many "bona fide" dynamic domains; hence, standard deviations for the relevant τ_c values could be easily calculated. Furthermore, close inspection of the $[I^*(\lambda_c)]^2$ distributions showed that, beside the main peaks, "baseline" values are seldom null, and that some peaks occurring in the τ_c spectra are very "small". One could question how much information is truly contained in the baseline and minor peaks. Therefore, a further criterion was needed to decide whether a peak is really significant or should be rather considered as a sort of background noise. We can reasonably suggest that a peak should be accepted as carrying real information if it provides, for at least one experimental point, a contribution larger than the relevant uncertainty. We verified that in all the cases examined herein, the contribution from the baseline is always below the significance limit proposed, whereas all the identified peaks satisfy the aforementioned criterion.

At this point, a detailed analysis of the whole results provides a reasonable support to the idea that the dynamic domains, identified by the heuristic procedure, actually mirror some microscopic features of the samples. Starting from native β-cyclodextrin (Figure 1), the $[I^*(\lambda_c)]^2$ distribution features a set of three main delta peaks centered at τ_c values of 1.66 ± 0.25 μs, 250 ± 40 ns, 9.5 ± 3.3 ns. A fourth peak at 66 ns, which does not individuate a cluster in the Monte-Carlo simulation, can be reasonably considered an artifact. These results immediately lead back to the possible molecular motion modes occurring in the system, i.e.: *i*) the oscillation of the mass centers of the cyclodextrin units in the crystalline lattice, *ii*) the torsion and tilting movements[15] of subsequent glucose units around α-glycosidic bridges within the oligosaccharide structure, *iii*) the rotation of the $-CH_2OH$ groups of the glucose units, respectively. It is worth noting that the occurrence of a null R_0 value, indicating the existence of no "fast" dynamic domains (τ_c < 1 ns), is consistent with the idea that the $-CH_2OH$ rotation is significantly slowed down by effective hydrogen bonding occurring in the lattice.

The nanosponge, the Parmigiano Reggiano cheese and the water-saturated cellulose samples offered the opportunity to test our heuristic-model analysis on some

complex systems, such as a natural or artificial polymer or a dairy product complex matrix. On one hand, the choice of the cheese sample allows a suitable comparison with the results obtained with the original Kruk's approach. On the other hand, β-cyclodextrin, nanosponge and cellulose are interesting because they constitute a set of chemically homogeneous systems.

For the dry nanosponge sample a more complex situation occurs (Figure 2) in comparison to β-cyclodextrin. This is consistent with the fact that the system becomes stiffer and more disordered owing to reticulation. Indeed, the τ_c value for the slowest domain increases up to 2.6 ± 1.0 μs (a further minor artifact component appears at 4.6 μs). The τ_c values for the intermediate domains (250 ± 120 and 69 ± 10 ns) seem hardly affected by reticulation. By contrast, even the fastest domain slows down (with τ_c = 30 ± 6 ns) and a significant offset component (R_0 = 3.3 ± 0.8 s^{-1}) appears. The latter findings are justified by the reticulated and disordered structure of the polymeric material. In fact, the $-CH_2OH$ groups involved in the reaction with the reticulating agent are unable to freely rotate. Conversely, unreacted $-CH_2OH$ groups are less affected by hydrogen bond formation in the disordered structure of the nanosponge. At the same time, the possible fast conformational rearrangements of the hexamethylene linker chains must be also kept into account. Noticeably, the occurrence of a significant microscopic disorder is mirrored in the very large indeterminations values found.

Regarding the cheese sample, it is worth preliminary mentioning that an average weight content of ca. 30 % in water, 34 % in proteins and 28 % in fats can be assumed.[4] Analysis of the relevant τ_c spectrum (Figure 3) shows a substantial consistency with the results obtained by applying Kruk's equation 6, which provided: R_0 = 4.7 ± 0.6 s^{-1}, $\tau_{c,1}$ = 3.3 ± 0.5 μs, $\tau_{c,2}$ = 190 ± 10 ns, $\tau_{c,3}$ = 22 ± 4 ns.[4] In fact, on applying our heuristic method, the same R_0 value (4.3 ± 0.3 s^{-1}) was obtained within experimental uncertainties. Moreover, two main τ_c components at 18.2 ± 1.8 ns and 151 ± 9 ns were found. These are perfectly comparable with the aforementioned $\tau_{c,2}$ and $\tau_{c,3}$ values. According to literature,[3-4] these components can be conceivably related to the occurrence of fast motions pertaining to the water molecules embedded in the cheese matrix, and to the conformational rearrangements of the alkyl chains of both aminoacid residues and fats. Two further τ_c peaks at 0.8 ± 0.4 μs and 6.4 ± 2.4 μs (with a possible minor artifact at 29.5 μs) may be related to the slow motions of the macromolecular constituents. Good agreement between our results and those obtained with Kruk's equation can be also observed for the parameters relevant to the quadrupolar dips. In details, we found (in parentheses the corresponding values obtained with Kruk's equation): C^{NH} = 0.87 ± 0.03 (1.2 ± 0.2) ms^{-2}; τ_Q = 6.72 ± 0.15 (6.5 ± 0.9) μs; ω_+ = 2.83 ± 0.03 (2.82 ± 0.01) MHz; ω_- = 2.12 ± 0.04 (2.09 ± 0.03) MHz; Φ = 2.15 ± 0.02 (2.10 ± 0.03) rad; Θ = 4.7 ± 1.5 (5.3 ± 0.2) rad.

Finally, for the water saturated cellulose an R_0 value of 0.84 ± 0.11 s^{-1} and three main τ_c components can be found at 2.8 ± 1.4 μs, 460 ± 160 ns and 79 ± 10 ns (with a minor component at 22 ± 12 μs, Figure 4). Once again, the R_0 contribution may be attributed to water molecules motions, which are likely slower than in the cheese sample, due to the highly structuring effect of the hydroxylated polysaccharide backbone. The components at 79 and 460 ns may account for the rotation of the glucose $-CH_2OH$ units, and to the torsion and tilting movements of the glucose residues around the β-glycosidic bridges, respectively. All these movements appear to be slower than in the case of the cyclodextrin sample. This can be justified by considering the well-known occurrence of a stiffer hydrogen bonding network in cellulose, as compared to the amylose-related molecules where α-glycosidic bridges occur. The other components at long τ_c values may account for the slow translational motions of the macromolecular backbone.

In conclusion, we set up a heuristic analysis method of NMRD relaxometric curves. This consists in retrieving the relevant integral inverse transform (with the well-known BPP function as the kernel), by means of a suitable numerical integration. The main strength points in our analysis are: *i)* the fact that unlike ordinary "model-free" analysis methods, no element of discretion is introduced; *ii)* surprisingly, a τ_c values spectrum is achieved, thereby pointing out at the existence of well identified dynamic domains. The latter observation poses the question of how much physical significance can be attributed to the obtained τ_c values. After testing our heuristic-model analysis on some datasets for real samples, it seems that the τ_c components individuated may be actually related to some structural features. Of course, caution is needed in performing any attribution, as long as complex matrixes are considered. However, the results shown herein suggest that our analysis method reasonably seem of general applicability. Future work will be indeed needed (and is currently in progress) to gain further evidences and insights, in comparison with independent results from different techniques. As a final remark, we are also perfectly aware that the reliability and informativeness of the heuristic method proposed here critically depends on the inversion routine used. Our home-made procedure may indeed appear rudimentary (and probably is), and is largely liable of improvement. However, our final goal in proposing it as a new tool for the analysis of NMRD curves, was also to stimulate both a debate in the scientific community regarding the possibilities of free-model based analyses, and the search for a more rigorous and elegant mathematical approach.

Supporting Information

The Supporting Information is available free of charge on the ACS Publications website.

i) Further information on the implementation of the heuristic algorithm, *ii*) Experimental details and *iii*) Relaxometric data for the water-saturated commercial cellulose sample (PDF).

AUTHOR INFORMATION

Corresponding Author

* Prof. P. Lo Meo: e-mail paolo.lomeo@unipa.it. Prof. P. Conte: e-mail pellegrino.conte@unipa.it.

Author Contributions

The manuscript was written through contributions of all authors.

ACKNOWLEDGMENT

Prof. Rainer Kimmich (University of Ulm, Germany) is gratefully acknowledged for useful discussion and encouragement.

REFERENCES

1. (a) Conte, P., Chapter 10 Environmental Applications of Fast Field-cycling NMR Relaxometry. In *Field-cycling NMR Relaxometry: Instrumentation, Model Theories and Applications*, The Royal Society of Chemistry: 2019; pp 229-254; (b) Steele, R. M.; Korb, J. P.; Ferrante, G.; Bubici, S., New applications and perspectives of fast field cycling NMR relaxometry. *Magn. Reson. Chem.* **2016,** *54* (6), 502-509; (c) Kimmich, R.; Anoardo, E., Field-cycling NMR relaxometry. *Prog. Nucl. Magn. Reson. Spectrosc.* **2004,** *44* (3), 257-320; (d) Conte, P.; Lo Meo, P., Nuclear Magnetic Resonance with Fast Field-Cycling Setup: A Valid Tool for Soil Quality Investigation. *Agronomy* **2020,** *10* (7), 1040.

2. (a) Overbeck, V.; Schröder, H.; Bonsa, A.-M.; Neymeyr, K.; Ludwig, R., Insights into the translational and rotational dynamics of cations and anions in protic ionic liquids by means of NMR fast-field-cycling relaxometry. *PCCP* **2021,** *23* (4), 2663-2675; (b) Jayakody, N. K.; Fraenza, C. C.; Greenbaum, S. G.; Ashby, D.; Dunn, B. S., NMR Relaxometry and Diffusometry Analysis of Dynamics in Ionic Liquids and Ionogels for Use in Lithium-Ion Batteries. *J. Phys. Chem. B* **2020,** *124* (31), 6843-6856.

3. (a) Kruk, D.; Masiewicz, E.; Borkowska, A. M.; Rochowski, P.; Fries, P. H.; Broche, L. M.; Lurie, D. J., Dynamics of solid proteins by means of nuclear magnetic resonance relaxometry. *Biomolecules* **2019,** *9* (11); (b) Kruk, D.; Masiewicz, E.; Wojciechowski, M.; Florek-Wojciechowska, M.; Broche, L. M.; Lurie, D. J., Slow dynamics of solid proteins – Nuclear magnetic resonance relaxometry versus dielectric spectroscopy. *J. Magn. Reson.* **2020,** *314*, 106721.

4. Conte, P.; Cinquanta, L.; Lo Meo, P.; Mazza, F.; Micalizzi, A.; Corona, O., Fast field cycling NMR relaxometry as a tool to monitor Parmigiano Reggiano cheese ripening. *Food Res. Int.* **2020**, 109845.

5. (a) Wangsness, R. K.; Bloch, F., The Dynamical Theory of Nuclear Induction. *Phys. Rev.* **1953,** *89* (4), 728-739; (b) Ballari, M.; Bonetto, F.; Anoardo, E., NMR relaxometry analysis of lubricant oils degradation. *J. Phys. D: Appl. Phys.* **2005,** *38* (19), 3746-3750.

6. Bloembergen, N.; Purcell, E. M.; Pound, R. V., Relaxation Effects in Nuclear Magnetic Resonance Absorption. *Phys. Rev.* **1948,** *73* (7), 679-712.

7. (a) Goddard, Y.; Korb, J.-P.; Bryant, R. G., The magnetic field and temperature dependences of proton spin-lattice relaxation in proteins. *J. Chem. Phys.* **2007,** *126* (17), 175105; (b) Goddard, Y. A.; Korb, J.-P.; Bryant, R. G., Water molecule contributions to proton spin–lattice relaxation in rotationally immobilized proteins. *J. Magn. Reson.* **2009,** *199* (1), 68-74; (c) Korb, J.-P.; Van-Quynh, A.; Bryant, R., Low-frequency localized spin-dynamical coupling in proteins. *Comptes Rend. Acad. Sci. - Series IIC - Chem.* **2001,** *4* (11), 833-837.

8. (a) Halle, B., The physical basis of model-free analysis of NMR relaxation data from proteins and complex fluids. *J. Chem. Phys.* **2009,** *131* (22), 224507; (b) Halle, B.; Jóhannesson, H.; Venu, K., Model-Free Analysis of Stretched Relaxation Dispersions. *J. Magn. Reson.* **1998,** *135* (1), 1-13.

9. (a) Lo Meo, P.; Mundo, F.; Terranova, S.; Conte, P.; Chillura Martino, D., Water Dynamics at the Solid–Liquid Interface to Unveil the Textural Features of Synthetic Nanosponges. *J. Phys. Chem. B* **2020,** *124* (9), 1847-1857; (b) Di Vincenzo, A.; Russo, M.; Cataldo, S.; Milea, D.; Pettignano, A.; Lo Meo, P., Effect of pH Variations on the Properties of Cyclodextrin-Calixarene Nanosponges. *ChemistrySelect* **2019,** *4* (20), 6155-6161; (c) Di Vincenzo, A.; Piccionello, A. P.; Spinella, A.; Chillura Martino, D.; Russo, M.; Lo Meo, P., Polyaminoazide mixtures for the synthesis of pH-responsive calixarene nanosponges. *Beilstein J. Org. Chem.* **2019,** *15*, 633-641; (d) Spinella, A.; Russo, M.; Di Vincenzo, A.; Chillura Martino, D.; Lo Meo, P., Hyper-reticulated calixarene polymers: a new example of entirely synthetic nanosponge materials. *Beilstein J. Org. Chem.* **2018,** *14*, 1498-1507; (e) Cinà, V.; Russo, M.; Lazzara, G.; Chillura Martino, D.; Lo Meo, P., Pre- and post-modification of mixed cyclodextrin-calixarene co-polymers: A route towards tunability. *Carbohydr. Polym.* **2017,** *157*, 1393-1403; (f) Russo, M.; Saladino, M. L.; Chillura Martino, D.; Lo Meo, P.; Noto, R., Polyaminocyclodextrin nanosponges: Synthesis, characterization and pH-responsive sequestration abilities. *RSC Adv.* **2016,** *6* (55), 49941-49953; (g) Massaro, M.; Cina, V.; Labbozzetta, M.; Lazzara, G.; Lo Meo, P.; Poma, P.; Riela, S.; Noto, R., Chemical and pharmaceutical evaluation of the relationship between triazole linkers and pore size on cyclodextrin-calixarene nanosponges used as carriers for natural drugs. *RSC Adv.* **2016,** *6* (56), 50858-50866; (h) Lo Meo, P.; Lazzara, G.; Liotta, L.; Riela, S.; Noto, R., Cyclodextrin–calixarene co-polymers as a new class of nanosponges. *Polym. Chem.* **2014,** *5* (15), 4499-4510.

10. (a) Trotta, F., Cyclodextrin Nanosponges and their Applications. In *Cyclodextrins in Pharmaceutics, Cosmetics, and Biomedicine*, John Wiley & Sons, Inc.: 2011; pp 323-342; (b) *Nanosponges: Synthesis and Applications*. Wiley-VCH Verlag GmbH & Co. KGaA: Weinheim, Germany, 2019.

11. (a) Wilson, L. D.; Mohamed, M. H.; Berhaut, C. L., Sorption of aromatic compounds with copolymer sorbent materials containing β-cyclodextrin. *Materials* **2011,** *4* (9), 1528-1542; (b) Wilson, L. D.; Mohamed, M. H.; Headley, J. V., Surface area and pore structure properties of urethane-based copolymers containing β-cyclodextrin. *J. Colloid Interf. Sci.* **2011,** *357* (1), 215-222.

12. (a) Conte, P.; Ferro, V., Measuring hydrological connectivity inside a soil by low field nuclear magnetic resonance relaxometry. *Hydrol. Proces.* **2018,** *32* (1), 93-101; (b) Conte, P.; Ferro, V., Standardizing the use of fast-field cycling NMR relaxometry for measuring hydrological connectivity inside the soil. *Magn. Reson. Chem.* **2020,** *58* (1), 41-50.

13. (a) Barnea, N.; Efros, V. D.; Leidemann, W.; Orlandini, G., The Lorentz Integral Transform and its Inversion. *Few-Body Systems* **2010,** *47* (4), 201-206; (b) Efros, V. D.; Leidemann, W.; Orlandini, G.; Barnea, N., The Lorentz integral transform (LIT) method and its applications to perturbation-induced reactions. *J. Phys. G: Nucl. Part. Phys.* **2007,** *34* (12), R459-R528; (c) Glöckle, W.; Schwamb, M., On the Ill-Posed Character of the Lorentz Integral Transform. *Few-Body Systems* **2009,** *46* (1), 55-62.

14. (a) Alper, J. S.; Gelb, R. I., Standard errors and confidence intervals in nonlinear regression: comparison of Monte Carlo and parametric statistics. *J. Phys. Chem.* **1990,** *94* (11), 4747-4751; (b) Lo Meo, P.; D'Anna, F.; Gruttadauria, M.; Riela, S.; Noto, R., Thermodynamics of binding between α- and β-cyclodextrins and some p-nitro-aniline derivatives: reconsidering the enthalpy–entropy compensation effect. *Tetrahedron* **2004,** *60* (41), 9099-9111.

15. (a) French, A. D.; Johnson, G. P., Linkage and pyranosyl ring twisting in cyclodextrins. *Carbohydr. Res.* **2007,** *342* (9), 1223-1237; (b) Naidoo,

K. J.; Gamieldien, M. R.; Chen, J. Y.-J.; Widmalm, G.; Maliniak, A., Glucose Orientation and Dynamics in α-, β-, and γ-Cyclodextrins. *J. Phys. Chem. B* 2008, *112* (47), 15151-15157.

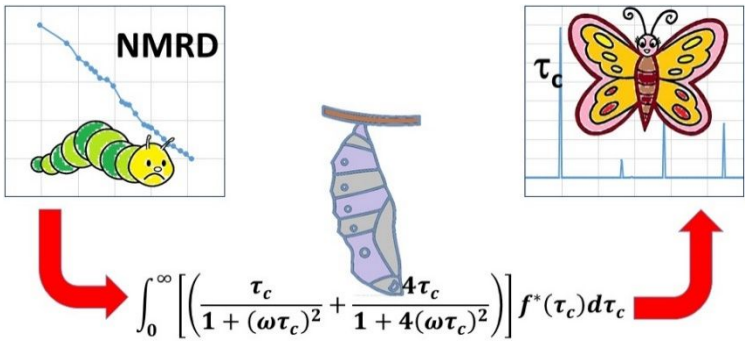

Insert Table of Contents artwork here

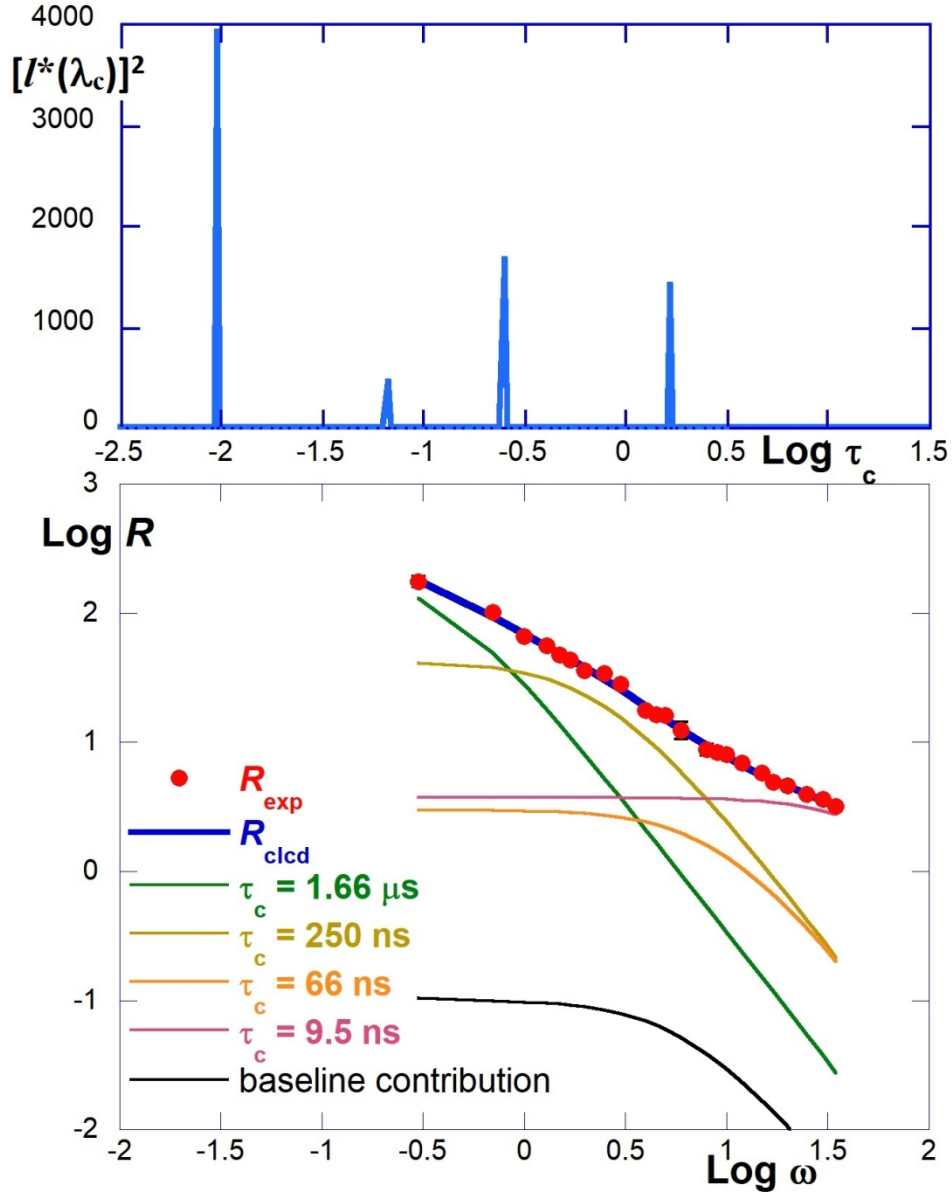

Figure 1. Spectrum of τ_C values (up) and NMRD curve (down) for the anhydrous β-cyclodextrin sample.

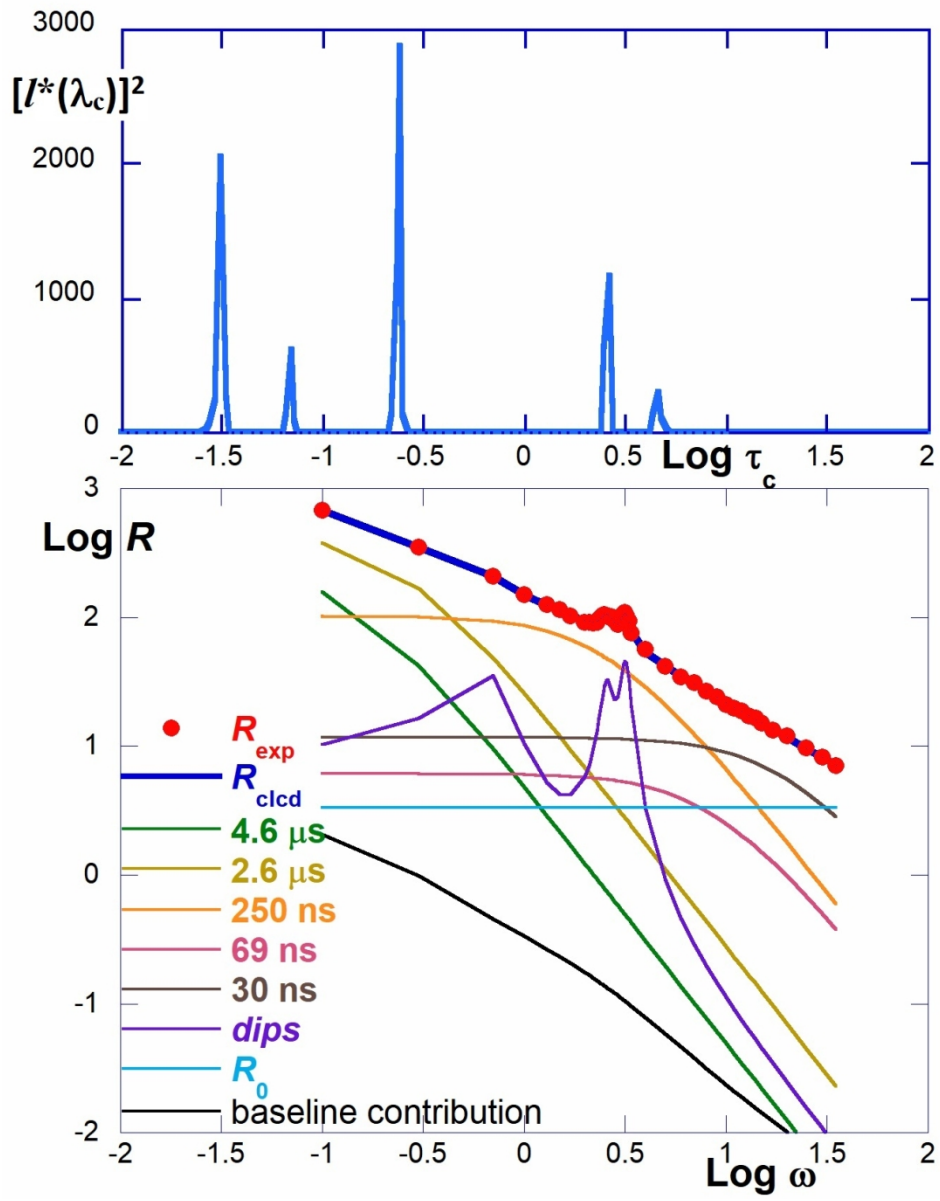

Figure 2. Spectrum of τ_C values (up) and NMRD curve (down) for the cyclodextrin-bis-urethane-based nanosponge sample.

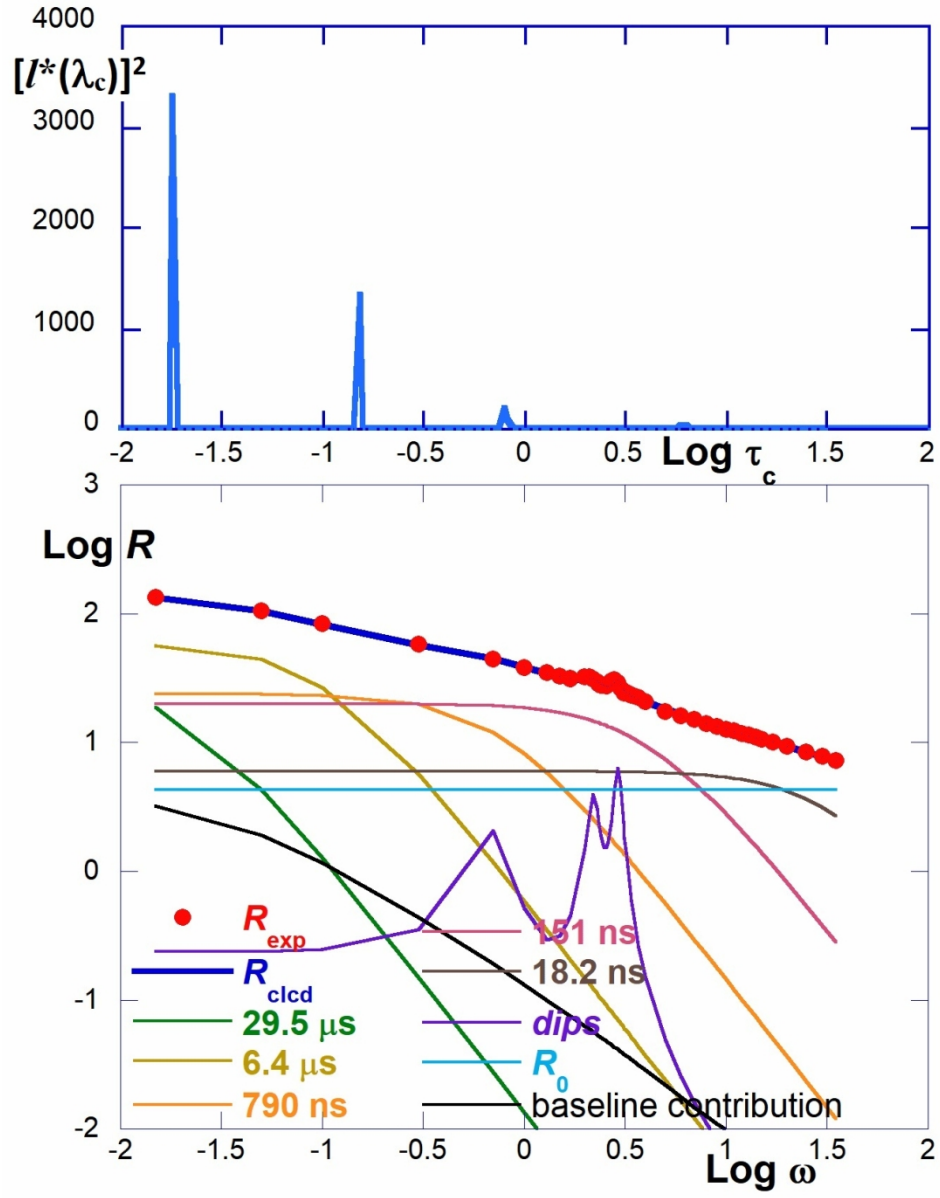

Figure 3. Spectrum of τ_C values (up) and NMRD curve (down) for the Parmigiano-Reggiano sample.

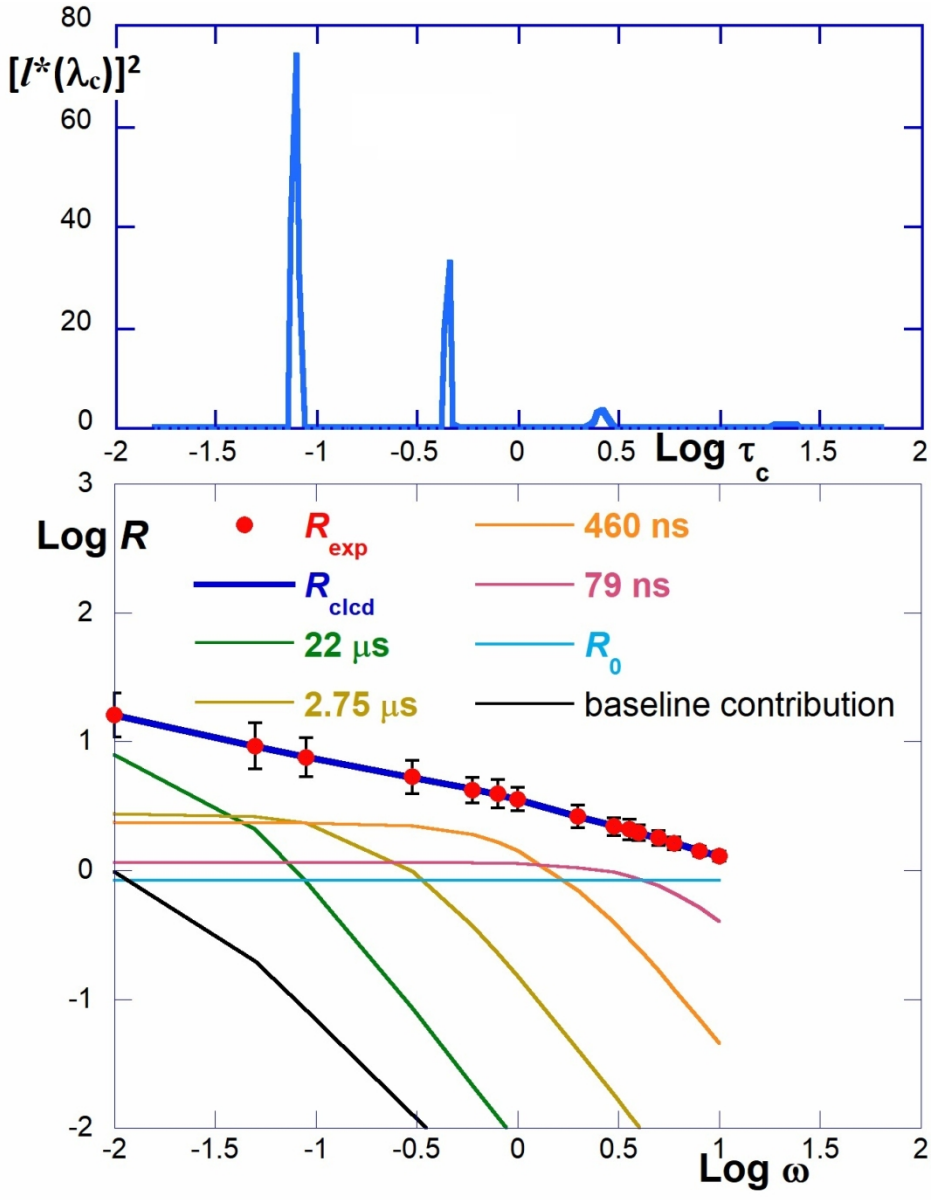

Figure 4. Spectrum of τ_C values (up) and NMRD curve (down) for the water saturated cellulose sample.

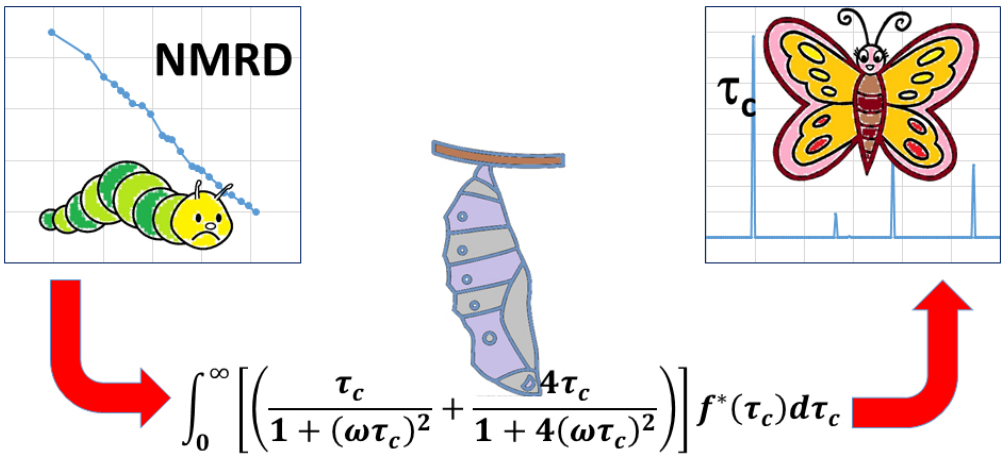

248x112mm (96 x 96 DPI)